Impurity Effects on Small Pd Clusters: A Relativistic Density Functional Study of Pd_4X, X = H, C, O

Alexander Genest, Sven Krüger, and Notker Rösch*

Department Chemie, Theoretische Chemie, Technische Universität München, 85747 Garching, Germany

Received: December 19, 2007; Revised Manuscript Received: February 22, 2008

We carried out relativistic density functional calculations to investigate systematically the effect of main group element impurities H, C, and O on a Pd_4 cluster. We determined a bridging coordination for Pd_4H as most stable, whereas several other local minima are energetically close. The interaction of C with Pd_4 is strong enough to restructure the cluster, resulting in two Pd_2 units bridged by 4-fold coordinated C, but other isomers are again almost degenerate. Nearly degenerate isomers of Pd_4O exhibit 2- and 3-fold coordination of O. In the most stable structures, the binding energies of the impurities, 295 kJ/mol for Pd_4H, 655 kJ/mol for Pd_4C, and 367 kJ/mol for Pd_4O, are large enough to allow bond breaking of common small molecules when they interact with an ensemble of Pd_4 clusters. Interestingly, the noteworthy relativistic effect on the properties of Pd_4 also affects the interaction with impurity atoms. Comparison with other metals reveals similarities with Ni_4X and differences from Ir_4H, Ir_4C, and Pt_4H.

Introduction

Palladium is widely used in industrial processes to activate hydrogen; thus, there is considerable interest in understanding the catalytic activity of this element.[1,2] Palladium clusters are used in catalytic hydrogenation, oxidation, and reduction of hydrocarbons.[3,4] A variety of experimental and theoretical studies addressed properties of Pd surfaces,[4,5] supported Pd clusters,[5,6] and Pd clusters in the gas phase.[4–10]

The structure of small metal clusters (in the gas phase or on a support) as well as their electronic and magnetic properties can be strongly affected by impurity atoms. Supported metal clusters can easily be contaminated by reactions with surface active sites (e.g., OH groups),[11,12] or the decomposition of molecular ligands (e.g., CO) adsorbed on the metal moiety.[13–17] From several computational studies it was concluded that supported metal clusters produced from carbonylated precursors are not free of heteroatoms.[11,12,14] Although impurity atoms can have a strong influence on the properties of metal clusters,[18–21] experimental information on the presence of heteroatoms and their influence on the clusters is very limited because controlled synthesis of such samples as well as their spectroscopic characterization present quite a challenge.[22]

Scarcity of experimental information motivated theoretical model studies of small transition metal clusters interacting with impurities. Single heteroatoms like H, C, and O were modeled as impurities at M_4 for M = Fe,[23–25] Co,[23] Ni,[26] Pd,[27,28] Pt,[29] and Ir.[30] Furthermore, coordination of two and more hydrogen ligands was studied for V,[31] Fe_4,[23] Co_4,[23] Cu_4,[27] Pd_4,[27] Pt_4,[29] and Ir_4.[33] These impurity atoms were selected not only for their importance in gas-phase chemistry of size selected clusters' but also with regard to heterogeneous catalytic systems where supported transition metal clusters often are utilized as components of active multifunctional catalysts.[34,35] The interaction of H and C atoms with Pd_4 clusters was studied with the hybrid B3LYP method, employing pseudopotentials.[4,27] A study on Pd_4H determined a distorted 3-fold coordination of the heteroatom as most stable,[27] whereas another one identified a bridging coordination at Pd_4 as most stable.[4] For Pd_4C a structure composed of two Pd_2 dimers oriented perpendicularly and bridged be the carbon atom was reported.[4] These earlier studies communicated only binding energies (BEs) and geometries but did not include the isomer spectrum of Pd_4X, although in one case searches for stable structures were started from several initial geometries.[27] To the best of our knowledge, Pd_4O has not yet been investigated computationally.

The present study focuses on how single impurity atoms affect the structure and other properties of the cluster Pd_4. We selected H, C, and O as heteroatoms because these main group elements are abundant in a variety of catalytic reactions, e.g., hydrogenation, oxidation, or reduction.[32] To contribute to the understanding of the effect of impurity atoms on small metal particles, we studied for the first time in a systematic fashion preferred binding sites, bond distances, energetics, the electronic structure, and the normal modes of Pd_4X, X = H, C, O, as well as the spectrum of low lying isomers, employing an accurate scalar relativistic density functional approach. As we applied an all-electron approach, we were able to inspect directly also relativistic effects. Comparison to M_4 clusters of other transition metals is facilitated by the fact that we used the same computational strategy as in previous studies on Ni_4X[26] and Ir_4H.[30] The results of the present study hopefully will help to identify pertinent species in experiments.

Method

We carried out all-electron calculations with the linear combination of Gaussian-type orbitals fitting-functions density functional method[36] (LCGTO-FF-DF) as implemented in the parallel quantum chemistry package ParaGauss.[37,38] Scalar relativistic effects were taken into account with the Douglas–Kroll–Hess (DKH) approach to the Kohn–Sham problem;[39–41] effects of spin-orbit interaction were neglected, but spin-polarization was admitted where appropriate. For the exchange-correlation functional we invoked the generalized gradient approximation (GGA) as suggested by Becke[42] and Perdew (BP86).[43] We used Gaussian-type basis sets in the form of

* Corresponding author. E-mail: roesch@ch.tum.de.

10.1021/jp7119075 CCC: $40.75
Published on Web 07/26/2008

TABLE 1: Properties of Pd_4X Complexes, X = H, C, O, As Determined by Scalar Relativistic Calculations[a]

	isomer[b]	sym[c]	BE	BE_0	BE_{nr}	Pd−X		<Pd−Pd>	q	M	IP	EA	config	
Pd_4H	μ_1	C_s	282	254	308	163	187	269	−0.23	2	6.81	1.41	$37a''^1$	
	μ_2-1	C_s	284	253	306	167	210	268	−0.23	2	7.17	1.41	$56a'^1$	
	μ_2-2	C_{2v}	295	262	305	165		266	−0.30	2	7.08	1.44	$56a'^1$	
	μ_2-3	C_s	279	249	302	163		265	−0.32	2	7.15	1.37	$56a'^1$	
Pd_4C	μ_3	C_s	634	624	609	190	191	272	−0.76	1	7.03	1.66		
	μ_4-1	D_{4h}	623	612	603	193		273	−1.14	3	6.65	1.94	$38a''^1$	$58a'^1$
	μ_4-2	C_s	644	633	619	189	191	283	−0.80	1	6.34	1.63		
	μ_4-3	D_{2d}	655	643	627	191		262	−0.74	1	6.44	1.63		
Pd_4O	μ_2	C_{2v}	367	360	356	193	193	267	−0.71	3	7.30	1.90	$59a'^1$	$38a''^1$
	μ_3	C_s	362	355	380	200	201	276	−0.64	3	7.05	1.64	$59a'^1$	$38a''^1$
Pd_4		D_{2d}	639[d]	644[d]	402[d]			261		3	6.72	1.31	$23e^2$	

[a] Symmetry (sym), binding energies BE, and binding energy BE_0 corrected for the zero point energy, Pd−X distances (the two shortest values), averaged Pd−Pd distances <Pd−Pd>, charge q(X) derived by fitting of the electrostatic potential, ground state spin multiplicity M, ionization potential (IP), electron affinity (EA), and orbital configuration (config), restricted to incompletely filled orbitals. Nonrelativistic binding energies BE_{nr} of the ligands X and results for tetrahedral Pd_4 (D_{2d}) are shown for comparison. Binding energies in kJ/mol, distances in pm, charges in e, IP and EA in eV. [b] Coordination mode of the heteroatom, extended by running label. See Figure 1. [c] Symmetry of geometry of the resulting structure; all calculations were performed with C_s symmetry constraints only. [d] For Pd_4 the atomization energy AE is quoted in place of BE.

atomic contractions. The basis set for Pd (18s13p9d) was contracted to [7s6p4d].[44] The basis sets for H, C, and O as well as other computational parameters, e.g., the auxiliary basis set for representing the electron density, were chosen as in a previous study.[26] Separate contractions for relativistic and nonrelativistic calculations were obtained from the corresponding atomic calculations. In all cases, we checked the Kohn−Sham determinant for spin contamination; deviations from the nominal value $S(S + 1)$ were at most 0.04.

We characterized all stationary points with a normal mode analysis; in the following, we will discuss only structures that represent local energy minima. To characterize the various structures, we use designators adopted from those in use for inorganic complexes:[26] μ_1 designates terminal coordination of the impurity X, μ_2 bridge, μ_3 hollow, and μ_4 4-fold coordination. We discriminate isomers of the same type of coordination by consecutive numbering, e.g., μ_2-n.

We scanned the configuration space of Pd_4X, starting from tetrahedral or square planar Pd_4. First, we optimized high-symmetry structures: tetrahedral $Pd_4(\mu_1$-X) in C_{3v}, $Pd_4(\mu_2$-X) in C_{2v}, $Pd_4(\mu_3$-X) in C_{3v}, $Pd_4(\mu_4$-X) in T_d, and the square planar structure $Pd_4(\mu_4$-X) in D_{4h} symmetry. Subsequently all these structures were slightly distorted and re-optimized in C_s symmetry. The stationary points obtained were then classified according to symmetry and confirmed by a normal mode analysis without symmetry constraints. To inspect relativistic effects, we also optimized geometries at the nonrelativistic level, starting from the structures obtained at the scalar relativistic level.

Ionization potentials (IP) and electron affinities (EA) were determined as differences of ground-state energies of the neutral and the corresponding ionic systems, calculated at the structure optimized for the neutral system. We assigned charges to the various atoms of Pd_4X by fitting the electrostatic potential.[45]

Results and Discussion

Pd_4. The bare cluster Pd_4 is known to be most stable as triplet, in a slightly distorted tetrahedral shape.[1,4,27,32,46–53] Average Pd−Pd bond lengths from GGA calculations of distorted tetrahedral structures were 261 pm and atomization energies (AE) ranged from 628 to 643 kJ/mol.[48,50] In agreement with earlier studies[2,4,32,46,48,50,51,53] we also calculated a triplet state with a marginally distorted tetrahedral structure (D_{2d}) as most stable isomer of Pd_4. The average Pd−Pd distance was 261 pm and the atomization energy 639 kJ/mol (Table 1); the latter value translates into a binding energy (BE) of 160 kJ/mol per atom. The zero point energy (ZPE) correction lowers the atomization energy by only 5 kJ/mol (in total). In line with our earlier study on Pd_4,[50] the atomization energy exhibits a sizeable relativistic effect: it increases by 237 kJ/mol (∼60 %) in comparison to a nonrelativistic calculation; concomitantly, the average bond length shrinks by 6 pm (see Supporting Information, Table S1) when calculated in scalar relativistic fashion. Yet, the effective atomic configuration, $s^{0.56}p^{0.09}d^{9.35}$ at the relativistic level, is only marginally affected. The 5s contribution, important for the cluster bonding, is larger by 0.05 e and the 4d contribution smaller by 0.06 e, as result of the relativistic stabilization of the Pd 5s orbital.[54] A further consequence, also reflected in the shorter Pd−Pd bond length at the relativistic level, is the relativistic reduction of the 5s radial expectation value of a Pd atom: 12 pm in configuration d^{10} and 8 pm in configuration d^9s^1. These values are much larger than the estimate of ∼3 pm for the relativistic reduction of the *effective* atomic radius as deduced from the relativistic effects on average Pd−Pd distances and on bonds Pd−X with heteroatoms (Table S1). The 4d shell expands only marginally, 1 pm, at the relativistic level.

Pd_4H. For hydrogen as impurity, structures with terminal and bridging coordination were calculated, all of them doublets (Table 1). The most stable structure μ_2-2 exhibits C_{2v} symmetry; the BE of the heteroatom is 295 kJ/mol. A slightly less stable structure (BE = 284 kJ/mol) with bridging hydrogen bent towards a face of the Pd_4 tetrahedron, μ_2-1, was obtained when starting from a 3-fold coordinated structure. To confirm these two μ_2 structures as different, we determined intermediate structures by restricted geometry optimizations and revealed a barrier of ∼8 kJ/mol. Different orders of occupied valence orbitals and different atomic charges of the H atom (by 0.1 e) provide further evidence for the existence of two distinct isomers (Table 1). In contrast to these structures with a bridging H atom, the structure μ_2-3 exhibits an H atom inserted in a Pd−Pd bond. The corresponding bridged Pd−Pd distances are 278 pm for μ_2-1, 277 pm for μ_2-2, but 311 pm for μ_2-3; the last distance is notably larger than typical Pd−Pd distances. With a BE of 279 kJ/mol, structure μ_2-3 is the least stable among the bridging structures of $Pd_4(\mu_2$-H) studied. Finally, we also obtained a distorted 3-fold coordination of H as a local minimum with a BE of 282 kJ/mol; that structure may be classified as $Pd_4(\mu_1$-H), as it features one short (163 pm) and two longer (187 pm)

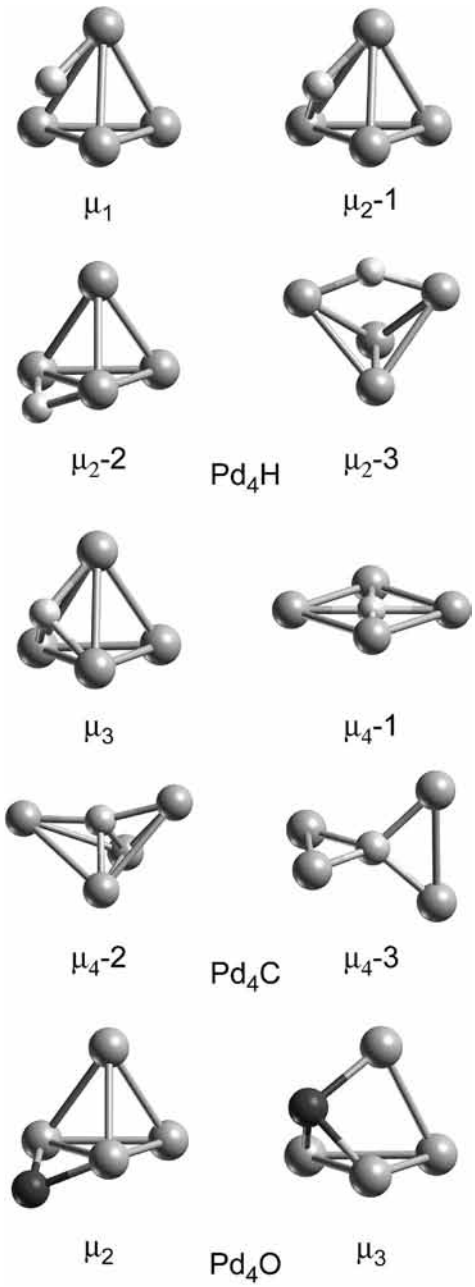

Figure 1. Calculated structures of various isomers of Pd_4X, X = H, C, and O.

Pd−H distances (Table 1). All calculated BEs of H at Pd_4 are large enough for dissociating H_2 (calculated BE 465 kJ/mol) according to the reaction $H_2 + 2Pd_4 \rightarrow 2Pd_4H$. Due to the rather high vibrational frequencies of H-related normal modes (see below), ZPE corrections reduce the binding energies by ∼30 kJ/mol but leave the relative stability of the isomers essentially unchanged (Table 1).

No systematic variations of the Pd−H bond lengths are observed among the isomers. These distances, 163 pm, are similar for terminal coordination and H inserted in a Pd−Pd bond. Somewhat larger values, up to 167 pm, were calculated for bridging H although the coordination number of the heteroatom does not change compared to the other structures. As BE(H) is larger than the energy per Pd−Pd bond in Pd_4 (107 kJ/mol), the average of Pd−Pd bonds of Pd_4H are longer, by up to 8 pm, compared to Pd_4.

All structures may be classified as hydrides as the H center is slightly negatively charged, −0.2 to −0.3 e (Table 1). Although the electron affinity is not affected by H coordination, the ionization potentials of the more stable structures were calculated somewhat larger than for Pd_4, by ∼0.4 eV (Table 1).

Whereas the IP and EA values are rather similar for all the isomers studied (Table 1), there may be a chance to identify the various isomers by the pattern of the H related vibrational frequencies (Table S2). For μ_1, we calculated a stretching mode of 2079 cm^{-1} and two lower bending modes, 1558 and 1119 cm^{-1}. The large frequency difference between the bending modes reflects the strongly tilted terminal coordination of H (Figure 1). For μ_2-1 and μ_2-2, stretching and frustrated bending modes along the bridge coordination site yield rather close frequencies (μ_2-1: 1965, 1928 cm^{-1}; μ_2-2: 2025, 2073 cm^{-1}, for stretching and bending modes, respectively). For the bending perpendicular to the bridged bond, we determined lower frequencies: 1144 cm^{-1} for μ_2-1 and 1210 cm^{-1} for μ_2-2. Compared to these rather similar spectra, μ_2-3 exhibits markedly different H related normal modes. The highest frequency, 2306 cm^{-1}, corresponds to an asymmetric stretching vibration along the bridged Pd−Pd bond. The two lower frequencies, 1488 and 1220 cm^{-1}, represent symmetric movements perpendicular to the bridged Pd−Pd bond: stretching and frustrated bending modes, respectively, of a conventional bridge coordinated structure. The normal modes of the Pd_4 moiety of 100−240 cm^{-1}, falling in the same range as for bare Pd_4, are not affected by H coordination (Table S2).

Two previous density functional studies, employing the B3LYP hybrid functional and the same pseudopotential approach, identified two different structures as ground state: either a complex with distorted 3-fold coordination of H,[27] similar to structure μ_1, or a bridge coordinated species[4] like μ_2-2 as the most stable structure of Pd_4H. For the distorted 3-fold coordinated structure a BE of 272 kJ/mol was calculated, slightly lower than our value of 284 kJ/mol. Concomitantly, also the shortest Pd−H bond (168 pm) was determined to be 5 pm longer than in the present work.[27] For the bridging structure μ_2-2, the two other studies reported lower BE values (259 kJ/mol,[4] 262 kJ/mol[27]) compared to the present value of 295 kJ/mol; this difference has to be attributed to the differences in the computational approaches. The relative order of Pd_4H isomers is easily affected even by small methodological details, as shown by the different ground states obtained in refs 4 and 27 with the same computational approach. However, all three investigations agree within 1 pm for the Pd−H distance. Overall, H prefers 2-fold coordination, but several energetically close lying isomers, as determined for the first time in this study, suggest that the species Pd_4H is quite flexible.

Pd_4C. For carbon, only structures with high coordination of the heteroatom were obtained. Opening Pd−Pd bonds of the tetrahedron with formal insertion of C leads to the most stable structures: C inserted in one Pd−Pd bond of the tetrahedron (μ_4-2; Figure 1) or two Pd_2 units bridged by the C atom (μ_4-3). Complexes with 4-fold coordination of C inside square planar Pd_4 (μ_4-1) and 3-fold coordination of C at a face of tetrahedral Pd_4 (μ_3) are somewhat less stable (Table 1).

The BE(C) values of all four species were calculated to be rather similar: μ_4-3, 655 kJ/mol; μ_4-2, 644 kJ/mol; μ_3, 634 kJ/mol; (planar) μ_4-1, 623 kJ/mol. ZPE corrections uniformly reduce these values by only 10–12 kJ/mol; this is considerably less than for Pd_4H due to the lower frequencies of the carbon related normal modes (Table S2). Despite their different topologies, all species exhibit rather similar Pd−C bond lengths, 189–191 pm; the planar structure μ_4-1 shows somewhat longer

bonds of 193 pm. For μ_3 the differences between the three Pd−C bonds is only 1 pm; thus, this structure exhibits essentially ideal μ_3 coordination with C_{3v} symmetry (Figure 1). Due to the low coordination of Pd atoms, the μ_4-3 structure yields a rather short average Pd−Pd distance, 262 pm, which is a nearest-neighbor distance due to the peculiar structure of this moiety. This value is similar to the average value of Pd_4 (261 pm), but 18 pm longer than in free Pd_2. For μ_3, a rather long average Pd−Pd distance resulted, 272 pm, reflecting the strong Pd−C interaction. A similar value, 273 pm, was obtained for the planar species μ_4-1; here, insertion of C strongly expands the square planar structure of Pd_4, for which Pd−Pd bonds of 242 pm were calculated. An even longer average Pd−Pd distance, 283 pm, was obtained for the structure μ_4-2.

All nonplanar structures of Pd_4C have a singlet ground state, and a charge of C of about −0.8 e (Table 1). Thus, the heteroatom of these structures can be assigned as carbidic. In contrast, the planar structure μ_4-1 exhibits a triplet ground state and an even stronger carbidic character, with $q(C) = -1.1$ e. The EA values of all nonplanar structures are about 0.3 eV larger than the EA of Pd_4. The planar structure μ_4-1 again deviated, with a larger change of 0.6 eV, resulting in an EA of 1.94 eV. The IPs of all structures with 4-fold coordinated carbon are lower than the IP of Pd_4, by up to 0.4 eV, whereas the IP of $Pd_4(\mu_3\text{-C})$ was calculated ∼0.3 eV larger than in Pd_4 (Table 1). Thus, as of Pd_4H, IP and EA values will be only of limited use for discriminating the various isomers of Pd_4C.

For μ_3 the three carbon related vibrational modes are rather close (625, 585, and 571 cm^{-1}, Table S2). In the planar structure μ_4-1, two in-plane modes of 717 cm^{-1} are well separated from the out-of-plane mode (355 cm^{-1}). Slightly larger frequencies were calculated for the open structures, which show a surprisingly similar pattern of the normal modes. The largest frequency of μ_4-2, 811 cm^{-1}, does not represent a stretching mode, but a vibration of the C atom parallel to the bond in which it is inserted. The two other modes are rather close in energy, 634 and 617 cm^{-1}. The μ_4-3 structure shows the same frequency pattern, with the higher frequency, 860 cm^{-1}, corresponding to an asymmetric stretching of the Pd_2−C bonds. Thus, especially the highest carbon related vibrational frequencies are characteristic for the different isomers and may be used for experimental differentiation.

An earlier density functional study, applying the B3LYP hybrid method in combination with pseudopotentials, also suggested the μ_4-3 structure as ground state of Pd_4C.[4] As for Pd_4H, the calculated BE(C), 528 kJ/mol,[4] was lower than the present GGA value of 655 kJ/mol. In line with the lower binding energy, Pd−C bonds obtained in that previous work (195 pm) were 4 pm longer[4] than in the present study.

Pd_4O. In the ground state of Pd_4O, the heteroatom bridges two Pd atoms, with BE(O) = 367 kJ/mol (Table 1; Figure 1). The Pd−O distances of this structure are 193 pm. The average Pd−Pd distance, 267 pm, is 6 pm longer than in bare Pd_4. Threefold coordinated O forms a complex of very similar energy, with BE(O) = 362 kJ/mol. In line with the higher coordination, it features longer Pd−O bonds of ∼200 pm together with elongated Pd−Pd distances, 276 pm on average. As for the other Pd_4X species, ZPE corrections (∼7 kJ/mol) of the binding energy do not affect the energetic ordering of the isomers of Pd_4O.

Both almost degenerate isomers are triplets, and the electron density transfer to oxygen is estimated to about −0.7 e; thus, the charge separation in Pd_4O is smaller than in Pd_4C (see above). IP and EA values of both structures of Pd_4O are larger than in Pd_4, by ∼0.3 and ∼0.6 eV for the structures μ_3 and μ_2, respectively.

Rather low vibrational frequencies of Pd_4O, compared to Pd_4C, go along with a kinetic energy contribution of the metal atoms to mainly O related vibrations. For both structures a stretching mode is calculated at ∼580 cm^{-1} (Table S2). The higher of the bending modes appear at 454 cm^{-1} for μ_2 and at 408 cm^{-1} for μ_3, whereas the corresponding lower modes yield frequencies of only 214 and 304 cm^{-1}, respectively. The lowest mode includes ∼25 % Pd contributions; its frequency, 214 cm^{-1}, falls below that of the highest metal mode, 224 cm^{-1}. Discrimination of the two isomers by vibrational spectroscopy would have to rely on identifying three (μ_2) or two (μ_3) modes above the Pd manifold.

Relativistic Effects. As revealed by nonrelativistic reoptimizations of all Pd_4X species, relativistic effects on structures are rather systematic (Table S1). In line with the relativistic change of the effective atom radius of Pd in Pd_4 by −3 pm, the average Pd−Pd distance contracts by ∼6 pm for all species Pd_4X. Accordingly, the relativistic results for Pd−X bonds are 2–4 pm shorter.

The relativistic increase of the *atomization energies*, obtained for all species Pd_4X, is dominated by the sizeable contribution from Pd_4, 237 kJ/mol, and scatters around that value by up to ∼30 kJ/mol. The relativistic changes of the *binding energies* of the heteroatom are not uniform. The scalar relativistic results for BE(H) are 10–26 kJ/mol smaller and those of BE(C) are 20–28 kJ/mol larger than the corresponding nonrelativistic results. The two Pd_4O isomers examined feature opposite relativistic effects in BE(O).

To analyze this nonuniform behavior, we decomposed the ligand binding energy into a deformation energy (activation) of the Pd_4 moiety to the structure adopted in Pd_4X and a binding energy of the ligand to that activated Pd_4 fragment. Only the first of the two energy contributions (20–50 kJ/mol for X = H, O; 40–200 kJ/mol for X = C; Table S1) exhibits a relativistic effect which reflects the relativistic strengthening of the Pd−Pd bonds. These relativistic increments are 10–30 kJ/mol for Pd_4H and Pd_4O and up to 60 kJ/mol for Pd_4C. For H, the strong pure ligand binding to the deformed Pd_4 moieties is only marginally affected by relativity (−9 to +2 kJ/mol). Relativistic effects increase the ligand binding to the deformed fragment slightly in the case X = O (10–25 kJ/mol), but notably in the case of carbon (50–85 kJ/mol). Thus, the small relativistic effects on the overall ligand binding energies BE mentioned above are the result of larger relativistic effects on two energy contributions of opposite sign, on fragment activation and ligand binding at that activated fragment.

Although relativistic effects on the binding energies are small, they do affect the isomer spectrum for H and O heteroatoms. At the nonrelativistic level (Table 1), all inspected Pd_4H isomers feature very similar ligand binding energies with the μ_1 complex being most stable. Thus, the ultimate preference for 2-fold coordination of H (Table 1) can be regarded as a relativistic effect. For Pd_4C, the μ_4-3 isomer is the most stable one at both levels of theory. Whereas Pd_4O prefers 3-fold coordination of O in the nonrelativistic model, 2- and 3-fold coordinated species exhibit very similar ligand binding energies when treated relativistically (Table 1).

Results of nonrelativistic calculations, carried out at the geometries optimized at the scalar relativistic level, closely agree with those determined for structures optimized at the nonrelativistic level (Table S1). All effects discussed above are only marginally affected by the relativistic geometry relaxation and

therefore can be classified as direct relativistic effects on the electronic structure of Pd_4 and Pd_4X.

Comparison to Tetramers of Other Metals. A study on Ni_4,[26] very similar to the present work on Pd_4, identified a hydrogen impurity to favor also bridging coordination. In contrast to Pd_4, only one local minimum was found. For Ni_5H the two most stable isomers show bridging H coordination.[55] Bridging coordination was also reported at tetrahedral Fe_4 and butterfly shaped Co_4.[23] In contrast, terminal H coordination was calculated to be preferred for Pt_4[29] and other Pt_n clusters[29] as well as for Ir_4,[30] whereas 2- and 3-fold coordination of hydride ligands is rather common in cluster compounds.[56]

The same computational strategy as applied here yielded structures of Ni_4C that are rather similar to those calculated for Pd_4C.[26] Threefold coordination of C on a Ni_4 tetrahedron and a slightly distorted central coordination in square planar Ni_4 are degenerate isomers, whereas insertion of C in a bond of tetrahedral Ni_4, the analog of $Pd_4(\mu_4\text{-}2)C$, is somewhat more stable.[26] A very similar structure was obtained for the most stable isomer of Ni_5C.[55] On the other hand, for Ni_4C no structure could be determined that resembles the most stable structure (μ_4-3) of Pd_4C. This may be rationalized by the stronger and shorter Ni−Ni bonds, which amount to 140 kJ/mol in tetrahedral Ni_4[26] compared to 106 kJ/mol for Pd_4. For Fe_4C, only distorted 3-fold coordination of C outside the Fe tetrahedron was reported.[24] For Ir_4C, μ_2 coordination of C to tetrahedral Ir_4 [similar to the structure of $Pd_4(\mu_2\text{-}3)H$] and to the most stable square-planar isomer of Ir_4 have been determined.[21] These results point towards marked differences between late elements of the first and second transition metal series on the one hand, and those of the third series on the other hand.

For Ni_4O only one μ_2 complex of the heteroatom was calculated,[26] whereas for Pd_4 complexes with 2- and 3-fold coordination feature very similar binding energies. For Ni_5O, on the other hand, an isomer with a distorted μ_3 coordination of oxygen was determined to be 20 kJ/mol more stable than the complex with bridging coordination.[55] For Fe_4O a bridging position was reported,[25] as for Ni_4O.[26] Therefore, one may expect tetramers of neighboring transition metals to show preferentially bridging O coordination.

Conclusions

We investigated computationally properties of Pd_4 clusters with H, C or O as typical impurity atoms that may occur under experimental conditions in catalytic reactions. We employed a scalar relativistic all-electron approach to account for relativistic effects which are important for transition metals of the second row.[50] Nonrelativistic calculations were performed to quantify relativistic effects.

We determined several close lying isomers of Pd_4H, with a preference for bridging coordination of H. This result is in line with an earlier density functional study,[4] whereas another study suggested a strongly distorted 3-fold coordinated structure as ground state.[27] In the present study, this latter structure was calculated to be only 13 kJ/mol less stable than the ground state. At the nonrelativistic level, μ_1 and μ_2 coordination of hydrogen to Pd_4 yielded essentially degenerate isomers. We determined four low-lying structures of Pd_4C within an energetic range of ~40 kJ/mol. In the two most stable structures, Pd−Pd bonds of tetrahedral Pd_4 are opened as result of the strong interaction with the C heteroatom. In the most stable structure of Pd_4C, at both levels of theory, two Pd_2 units sandwich the C center. For Pd_4O, 2- and 3-fold coordinated O positions were determined to be almost degenerate. In the nonrelativistic model, 3-fold coordination is preferred by 24 kJ/mol.

Relativistic effects result in shorter Pd−Pd and Pd-X bonds that can be rationalized by the smaller effective atomic radius of Pd. These uniform trends of bond distances are not matched by corresponding trends of binding energies BE(X) of the heteroatoms.

The binding energies of all heteroatoms are rather strong, increasing in the order H < O < C. They are sufficiently large to allow activation of small molecules like H_2, O_2, and CH_4 on an ensemble of Pd_4 clusters, when the final state is taken as a set of species Pd_4X. The bonds of CO and CO_2, on the other hand, are too strong to undergo dissociation in this way.

The structures of Pd_4X are quite similar to those of Ni_4X,[26] with the marked exception of the most stable structure of Pd_4C. The structures of M_4 (M = Fe, Co, and Ni) with an H impurity are quite similar to the bridging structure of Pd_4H, but Pt_4H[29] and Ir_4H[30] were calculated to prefer terminal coordination of the heteroatom.

Although structural parameters as well as IP and EA values of several of the isomers of the species inspected are rather similar, patterns of heteroatom-derived vibrational frequencies of Pd_4H and Pd_4C (and to some extent also of Pd_4O) differ notably among the various isomers and, thus, are well suited for experimental identification.

The collection of these data may help to establish trends among various transition metal species (especially when systematic studies of the same type are compared)[26,30] as well as to identify and discriminate various structures in experimental studies. The present results will also serve as convenient reference for identifying adsorption-induced effects on the properties of oxide-supported species.

Acknowledgment. This work was supported by Deutsche Forschungsgemeinschaft and Fonds der Chemischen Industrie (Germany).

Supporting Information Available: Table S1 with data for relativistic effects on properties of Pd_4X and Table S2 with the normal mode frequencies (in harmonic approximation) of all species studied. This material is available free of charge via the Internet at http://pubs.acs.org.

References and Notes

(1) Karpinski, Z. *Adv. Catal.* **1990**, *37*, 45.
(2) German, E. D.; Efremenko, I.; Sheintuch, M. *J. Phys. Chem. A* **2001**, *105*, 11312.
(3) Ciebien, J. F.; Cohen, R. E.; Duran, A. *Supramol. Sci.* **1998**, *5*, 31.
(4) Bertani, V.; Cavallotti, C.; Masi, M.; Carra, S. *J. Phys. Chem. A* **2000**, *104*, 11390.
(5) Yudanov, I. V.; Sahnoun, R.; Neyman, K. M.; Rösch, N. *J. Chem. Phys.* **2002**, *117*, 9887.
(6) Libuda, J.; Schauermann, S.; Laurin, M.; Schalow, T.; Freund, H.-J. *Monatsh. Chem.* **2005**, *136*, 59.
(7) Efremenko, I. *J. Mol. Catal. A* **2001**, *173*, 19.
(8) Astruc, D.; Lu, F.; Aranzaes, R. *Angew. Chem.* **2005**, *117*, 8062.
(9) Neyman, K. M.; Inntam, C.; Gordienko, A. B.; Yudanov, I. V.; Rösch, N. *J. Chem. Phys.* **2005**, *122*, 174705.
(10) Yudanov, I. V.; Sahnoun, R.; Neyman, K. M.; Rösch, N.; Hoffmann, J.; Schauermann, S.; Johánek, V.; Unterhalt, H.; Rupprechter, G.; Libuda, J.; Freund, H.-J. *J. Phys. Chem. B* **2003**, *107*, 255.
(11) Vayssilov, G. N.; Gates, B. C.; Rösch, N. *Angew. Chem. Int. Ed.* **2003**, *42*, 1391.
(12) Vayssilov, G. N.; Rösch, N. *Phys. Chem. Chem. Phys.* **2005**, *7*, 4019.
(13) Vajda, S.; Wolf, S.; Leisner, T.; Busolt, U.; Wöste, L. H.; Wales, D. *J. Chem. Phys.* **1997**, *107*, 3492.
(14) Goellner, J. F.; Neyman, K. M.; Mayer, M.; Nörtemann, F.; Gates, B. C.; Rösch, N. *Langmuir* **2000**, *6*, 2736.
(15) Alexeev, O.; Gates, B. C. *Top. Catal.* **2000**, *10*, 273.
(16) Armentrout, P. B. *Annu. Rev. Phys. Chem.* **2001**, *52*, 423.

(17) Pedersen, D. B.; Rayner, D. M.; Simard, B.; Addicoat, M. A.; Buntine, M. A.; Metha, G. F.; Fielicke, A. *J. Phys. Chem. A* **2004**, *108*, 964.
(18) Ferrari, A. M.; Neyman, K. M.; Mayer, M.; Staufer, M.; Gates, B. C.; Rösch, N. *J. Phys. Chem. B* **1999**, *103*, 5311.
(19) Petrova, G. P.; Vayssilov, G. N.; Rösch, N. *Chem. Phys. Lett.* **2007**, *444*, 215.
(20) Petrova, G. P.; Vayssilov, G. N.; Rösch, N. *J. Phys. Chem. C* **2007**, *111*, 14484.
(21) Stevanovic, V.; Sljivancanin, Z.; Baldereschi, A. *Phys. Rev. Lett.* **2007**, *99*, 165501.
(22) Li, F.; Yu, P.; Hartl, M.; Daemen, L. L.; Eckert, J.; Gates, B. C. *Z. Phys. Chem.* **2006**, *220*, 1553.
(23) Jones, N. O.; Beltran, M. R.; Khanna, S. N.; Baruha, T.; Pederson, M. R. *Phys. Rev. B* **2004**, 165406.
(24) Gutsev, G. L.; Mochena, M. D.; Bauschlicher, C. W., Jr. *J. Phys. Chem. A* **2004**, *108*, 11409.
(25) Gutsev, G. L.; Bauschlicher, C. W., Jr.; Zhai, H.-J.; Wang, L.-S. *J. Chem. Phys.* **2003**, *119*, 11135.
(26) Petkov, P.; Vayssilov, G.; Krüger, S.; Rösch, N. *Phys. Chem. Chem. Phys.* **2006**, *8*, 1282.
(27) Bertin, V.; Cruz, A.; del Angel, G.; Castro, M.; Poulain, E. *Int. J. Quantum Chem.* **2005**, *102*, 1092.
(28) Efremenko, I.; German, E. D.; Sheintuch, M. *J. Phys. Chem. A* **2000**, *104*, 8089.
(29) Sebetci, A. *Chem. Phys.* **2006**, *331*, 9.
(30) Bussai, C.; Krüger, S.; Vayssilov, G. N.; Rösch, N. *Phys. Chem. Chem. Phys.* **2005**, *7*, 2656.
(31) Swart, I.; Fielicke, A.; Redlich, B.; Meijer, G.; Weckhuysen, B. M.; de Groot, F. M. F. *J. Am. Chem. Soc.* **2007**, *129*, 2516.
(32) Moc, J.; Musaev, D. G.; Morokuma, K. *J. Phys. Chem. A* **2000**, *104*, 11606.
(33) Krüger, S.; Bussai, C.; Genest, A.; Rösch, N. *Phys. Chem. Chem. Phys.* **2006**, *8*, 3391.
(34) Ertl, G.; Knözinger, H. In *Handbook of Heterogeneous Catalysis*; Weitkamp, J., Ed.; Vol. 2; Wiley-VCH: Weinheim, 1997.
(35) Hadjiivanov, K. I.; Vayssilov, G. N. *Adv. Catal.* **2002**, *47*, 307.
(36) Dunlap, B. I.; Rösch, N. *Adv. Quantum Chem.* **1990**, *21*, 317.
(37) Belling, T.; Grauschopf, T.; Krüger, S.; Mayer, M.; Nörtemann, F.; Staufer, M.; Zenger, C.; Rösch, N. In *High Performance Scientific and Engineering Computing,* Lecture Notes in Computational Science and Engineering; Bungartz, H.-J., Durst, F., Zenger, C., Eds.; Springer: Heidelberg, 1999; Vol. 8, p 439.
(38) Belling, T.; Grauschopf, T.; Krüger, S.; Nörtemann, F.; Staufer, M.; Mayer, M.; Nasluzov, V. A.; Birkenheuer, U.; Hu, A.; Matveev, A. V.; Shor, A. M.; Fuchs-Rohr, M.; Neyman, K.; Ganyushin, D. I.; Kerdcharoen, T.; Woiterski, A.; Gordienko, A.; Majumder, S.; Rösch, N., PARAGAUSS, version 3.0; Technische Universität München, 2004.
(39) Häberlen, O. D.; Rösch, N. *Chem. Phys. Lett.* **1992**, *199*, 491.
(40) Rösch, N.; Krüger, S.; Mayer, M.; Nasluzov, V. A. In *Recent Developments and Applications of Modern Density Functional Theory*; Seminario, J., Ed.; Theoretical and Computational Chemistry, Vol. 4; Elsevier: Amsterdam, 1996; p 497.
(41) Rösch, N.; Matveev, A. V.; Nasluzov, V. A.; Neyman, K. M.; Moskaleva, L.; Krüger, S. In *Relativistic Electronic Structure Theory-Applications*; Schwerdtfeger, P., Ed.; Theoretical and Computational Chemistry Series, Vol. 14; Elsevier: Amsterdam, 2004; p 656.
(42) Becke, A. D. *Phys. Rev. A,* **1988**, *38*, 3098.
(43) (a) Perdew, J. P. *Phys. Rev. B* **1986**, *33*, 8822. (b) Perdew, J. P. *Phys. Rev. B* **1986**, *34*, 7406.
(44) Huzinaga, S. *J. Chem. Phys.* **1977**, *66*, 4245.
(45) Besler, B. H.; Merz, K. M.; Kollman, P. A. *J. Comput. Chem.* **1990**, *11*, 431.
(46) Valerio, G.; Toulhoat, H. *J. Phys. Chem.* **1996**, *100*, 10827.
(47) Fahmi, A.; van Santen, R. A. *J. Phys. Chem.* **1996**, *100*, 5676.
(48) Nava, P.; Sierka, M.; Ahlrichs, R. *Phys. Chem. Chem. Phys.* **2003**, *5*, 3372.
(49) Futschek, T.; Marsman, M.; Hafner, J. *J. Phys.: Condens. Matter.* **2005**, *17*, 5927.
(50) Xiao, C.; Krüger, S.; Belling, T.; Mayer, M.; Rösch, N. *Int. J. Quantum Chem.* **1999**, *74*, 405.
(51) Zacarias, A. G.; Castro, M.; Tour, J. M.; Seminario, J. M. *J. Phys. Chem. A* **1999**, *103*, 7692.
(52) Dai, D.; Balasubramanian, K. *J. Chem. Phys.* **1995**, *103*, 648.
(53) Zhang, W.; Ge, Q.; Wang, L. *J. Chem. Phys.* **2003**, *118*, 5793.
(54) Pyykkö, P. *Chem. Rev.* **1988**, *88*, 563.
(55) St. Petkov, P.; Vayssilov, G. N.; Krüger, S.; Rösch, N. *J. Phys. Chem. A* **2007**, *111*, 2067.
(56) Mingos D. M. P.; Wales D. J. *Introduction to Cluster Chemistry*; Prentice-Hall: Englewood Cliffs, 1990; Chapter 1.9.

JP7119075